

## Supplementary material for “Long wave propagation and run-up in converging bays”

Takenori Shimozone

In order to validate the estimated limit  $\mu_c = \sqrt{2q}$  in Section 4.1, the analytical solutions are compared with numerical results from the two-dimensional nonlinear shallow water equations, (2.1), (2.2) and (2.3). The model equations are discretized on a regular grid, and integrated by the MacCormack scheme. The computational domain consists of the converging bay connected to the uniform region which is much longer than the incident wavelength. The three bay types ( $q = 2, 1$  and  $2/3$ ) with  $l_y/l_x = 0.5$  and  $h_0/l_x = 0.1$  are taken up for the validation. A monochromatic wave is given at the end of the uniform region towards the bay, until a resulting standing wave in the bay reaches a nearly equilibrium state. For comparisons with the linear solutions, the ratio of incident wave amplitude to water depth is set to be very small ( $a_0/h_0 = 0.001$ ). The computation is carried out for three different values of  $\mu$  around the estimated limit:  $\mu/\mu_c = 0.5, 1.0$  and  $1.5$ . The grid spacing is set as  $\Delta x/l_x = \Delta y/l_x = 0.01$  for the V-shaped and U-shaped bays ( $q = 2, 1$ ), while  $\Delta x/l_x = \Delta y/l_x = 0.005$  for the cusped bay ( $q = 2/3$ ) to represent the rapid transition of the cross-section.

**Figure S1, S2 and S3** show the comparisons of wave amplitude distribution ( $a/a_0$ ) for the three bay types, respectively. In each figure, the upper panels represent the analytical results for the three  $\mu$  values, while the lower panels represent the corresponding numerical results. When  $\mu$  is well below the limit ( $\mu = 0.5 \mu_c$ ), the two results show good agreement. There are small discrepancies on the bay side, because the longitudinal transition of the cross-section is smoothly represented by the regular grid, especially for the strongly converging case ( $q = 2/3$ ). When  $\mu$  reaches the estimated limit ( $\mu = 1.0 \mu_c$ ), the analytical solutions slightly deviate from the numerical results. The minor discrepancies are due to the truncation errors of the analytical solutions. When  $\mu$  exceeds the limit ( $\mu = 1.5 \mu_c$ ), the analytical solutions are completely different from the numerical results. Beyond the limit, the numerical result depends on the length of the uniform region, because the wave amplitude longitudinally decays as a result of strong wave refraction.

These comparisons support the validity of the estimated limit and the related discussions in Section 4.1. The analytical solutions are confirmed to be valid close to the limit. The higher-order effect due to wave refraction rapidly grows beyond the limit, and the incident wave does not propagate as a progressive wave in the uniform region. The occurrence of this phenomenon cannot be described by the present solutions based on the assumption of weak transverse flows.

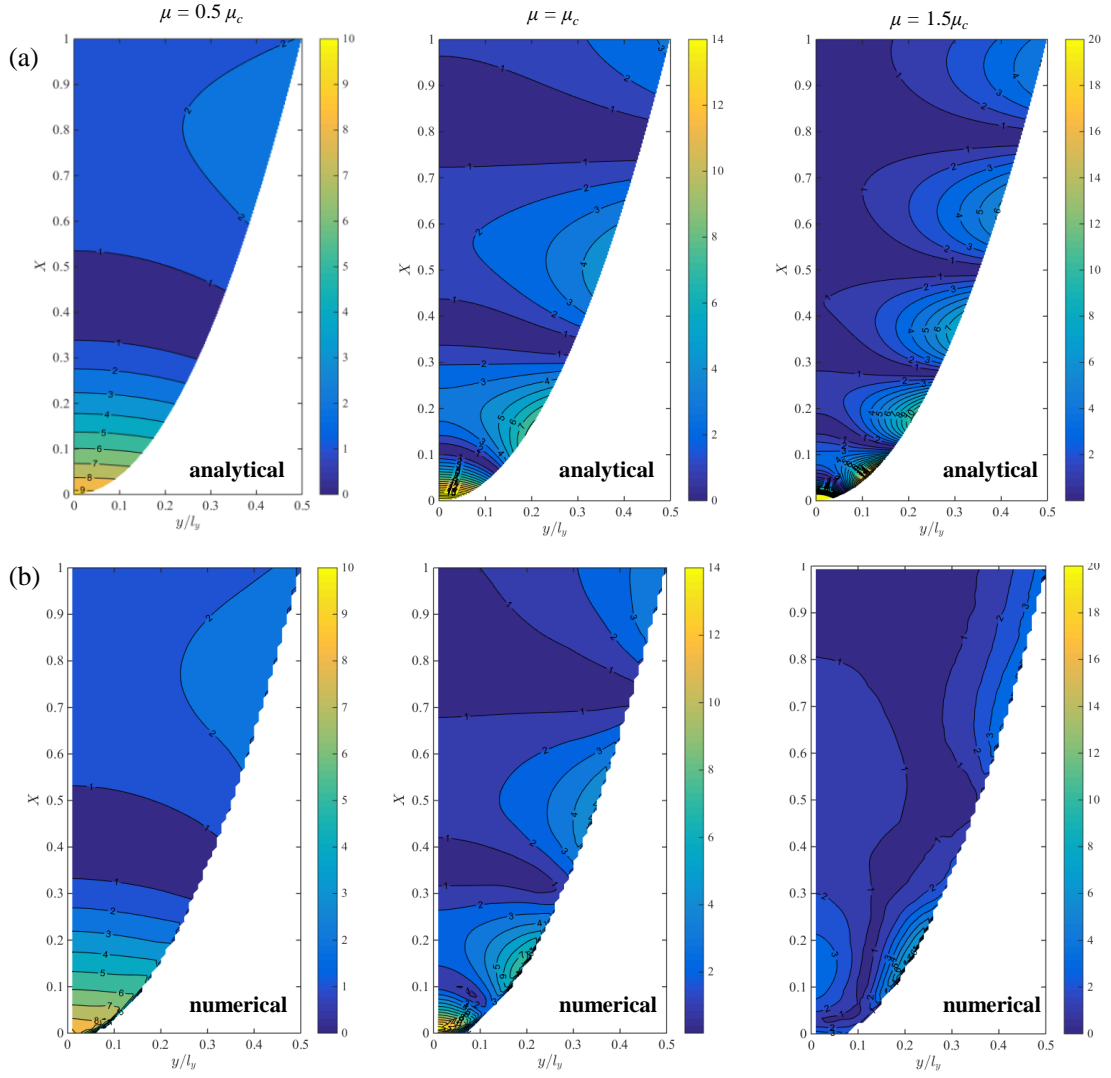


**Figure S1.** Analytical and numerical results of wave amplitude distribution inside the U-shaped bay for the three different  $\mu$  values. (a) Analytical results, (b) Numerical results.

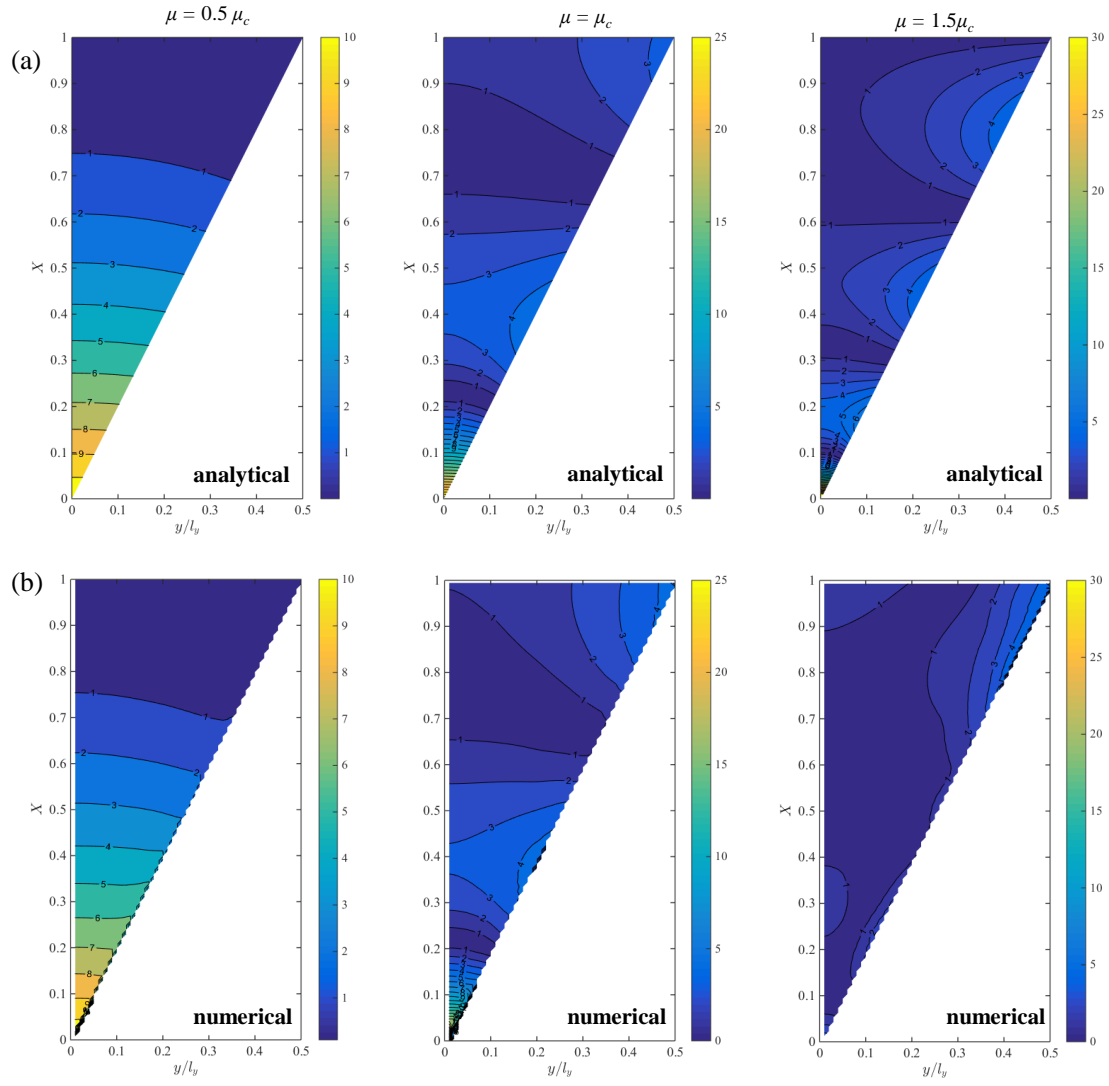


**Figure S2.** Analytical and numerical results of wave amplitude distribution inside the V-shaped bay for the three different  $\mu$  values. (a) Analytical results, (b) Numerical results.

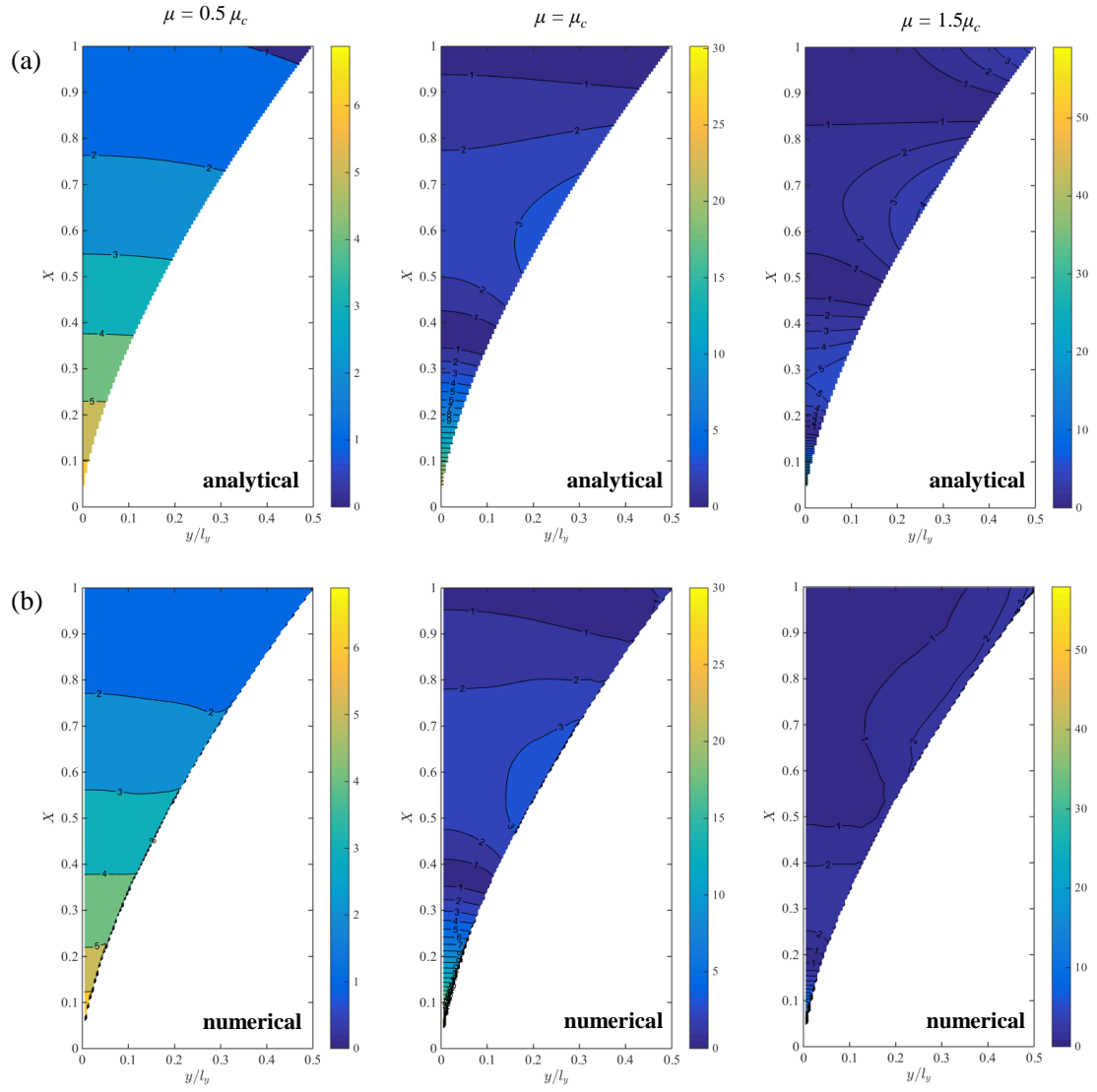


**Figure S3.** Analytical and numerical results of wave amplitude distribution inside the cusped bay for the three different  $\mu$  values. (a) Analytical results, (b) Numerical results.